Predistortion Linearizer Using GaAs Dual-Gate MESFET for TWTA and SSPA Used in Satellite Transponders

MAHESH KUMAR, SENIOR MEMBER, IEEE, JAMES C. WHARTENBY, MEMBER, IEEE, AND HERBERT J. WOLKSTEIN, SENIOR MEMBER, IEEE

Abstract—**Present traveling-wave tube amplifiers (TWTA) and solid-state power amplifiers (SSPA) used in communication systems both at ground stations and on-board satellites should be highly efficient and provide linear amplification. The performance of these microwave power amplifiers is limited, however, by intrinsic nonlinearities which result in undesirable distortions. In this paper, a new predistortion technique using GaAs dual-gate MESFET's is presented to linearize the TWTA's and SSPA's. The results of a *Ku*-band (11.7–12.2 GHz) linearized 16-W TWTA and *C*-band (3.8–4.2 GHz) linearized SSPA are presented.**

I. Introduction

INFORMATION-HANDLING capacity of current communication satellites is limited by nonlinearities in microwave power amplifiers (MPA) used in satellite transponders. These amplifier nonlinearities of the signal being relayed by the satellites lead to such undesirable effects as crosstalk, intermodulation distortions, reduced signal-to-noise ratio in the presence of multiple signals, etc. In order to reduce the nonlinearities of the signal generated in the MPA's and obtain higher carrier to third-order intermodulation distortion (C/3rd IMD) products ratios, amplifiers are operated well below saturation with consequent loss of efficiency and reduced power output and traffic handling capability.

A typical TWTA/SSPA RF power output versus RF power input is fairly linear in the small-signal region, and becomes quite nonlinear as the MPA is driven to saturation. These nonlinearities produce distortion products such as AM-to-AM conversion, AM-to-PM conversion, harmonics, and intermodulation products.

In the small-signal region, AM-to-AM conversion is nearly 1 dB/dB. At saturation, the AM-to-AM conversion becomes 0. Most AM communication systems require at least 0.9 dB/dB of AM-to-AM conversion, so that the MPA's output power must be backed off at least 6 to 8 dB for the TWTA and 2 to 3 dB for the SSPA from saturation.

The second type of distortion AM-to-PM conversion is a measure of the changes in MPA phase length resulting from changes in the RF power input and is defined as the slope of the phase versus the RF power input curve (degrees per decibel). The maximum allowable slope for many communication systems usually occurs at an RF input 3–6 dB below the level that causes saturation.

Another form of distortion in the MPA's is harmonic output power. When the MPA's are driven to saturation, the harmonics are generated because of the nonlinearities. Some of the power is converted into the harmonics as the MPA is driven near saturation and the efficiency of the amplifier reduces.

Nonlinearities in a MPA lead to the formation of mixing products when two or more signals are amplified by the MPA. These mixing products are called intermodulation distortion (IMD) products. The most important of these are the third-order IMD products, which results from the second-order distortion products of one signal mixing with the first-order products of another signal. The third-order IMD products are closer to the signal frequencies and larger in amplitude than the higher order products.

Fig. 1 shows the amplitude and phase transfer characteristics of a typical TWTA (solid curves). It is apparent that the amplitude curve is nonlinear and that the phase of the TWTA varies about 45°. In an ideal case, one would like to have constant gain with no change in phase as the input power is backed-off from saturation. The dotted curves shown for amplitude and phase represent the performance that can be expected with linearization. Obviously, the linearity of the MPA's can be greatly improved by using a linearization technique presented in this paper.

In this paper, we present a new technique of predistorting the input signal to the TWTA/SSPA, using dual-gate MESFET's. The circuit is quite simple and employs fewer components than do other predistortion techniques reported in the literature. The test results for a linearized *Ku*-band (11.7–12.2 GHz) 16-W TWTA and a linearized *C*-band (3.8–4.2 GHz) 12-W SSPA are presented.

II. System Aspects of the Linearizer

The purpose of a linearizer is to reduce the level of third-order intermodulation products in FDMA communication systems. In TDMA systems, the purpose of linearization is to reduce the intersymbol interference due to nonlinearity of the MPA and to reduce the spectrum

Manuscript received February 22, 1985; revised May 22, 1985.

M. Kumar and H. J. Wolkstein are with RCA Laboratories, David Sarnoff Research Center, Princeton, NJ 08540.

J. C. Whartenby was with RCA Laboratories, David Sarnoff Research Center. Presently, he is with MSC, Somerset, NJ.

0018-9480/85/1200-1479$01.00 ©1985 IEEE

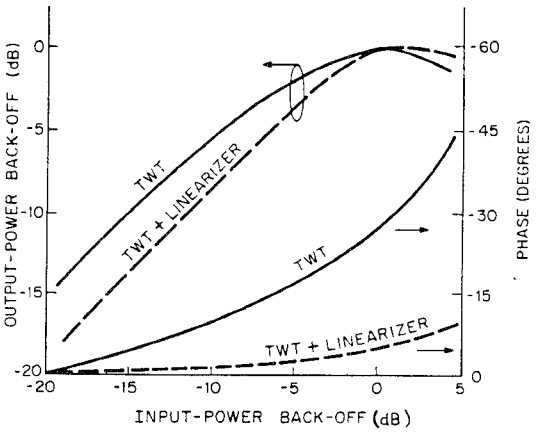

Fig. 1. A typical amplitude and phase transfer characteristics of a TWTA and linearized TWTA.

spreading at the output of the MPA. Spectrum spreading generates strong interferences in adjacent channels. In both systems, linearization will reduce the need for MPA output power back-off and thus improves both the performance and the efficiency of the system.

III. Various Techniques of Linearization

There are many methods for improving the linearity of the TWTA's, namely, feedforward [1], negative feedback [2], [3], and predistortion [4]–[12]. Feedforward is an attractive approach that has been widely used. However, two MPA's and ancilliary power supplies are required. The feedforward system also requires that the absolute phase for each MPA be constant to within a few degrees. The requirement of another MPA in the auxilliary arm reduces the efficiency of the system and the circuitry involved is quite complex. Therefore, this technique is not suitable for use within the satellite; however, it is an accepted technique for use in the less constrained ground station.

The negative feedback technique requires special treatment of the time delay [2] and bandwidth involved [3]. Because of the several cycles of delay required between input to output, the bandwidth obtained by this technique is quite narrow. However, for a narrow-band application, this may be a practical way of achieving linearity.

The predistortion technique has been widely used to linearize MPA's using Schottky diodes and MESFET's (in saturation) as nonlinear elements and distortion generators. This scheme in general, provides both broad frequency bandwidth and wide dynamic range. To accomplish this, inverse distortions, both in amplitude and phase, are generated and summed with the MPA input to cancel nonlinearities within the MPA.

IV. Principle of Operation

There are two sources of nonlinearities in the microwave power amplifier: a) amplitude nonlinearity and b) phase nonlinearity. The intermodulation distortions generated by phase nonlinearity is orthogonal to that generated by amplitude nonlinearity. Therefore, a linearizer should be capable of generating both inverse amplitude and phase nonlinearities to achieve a substantial reduction in the IMD products. Fig. 2(a) is a schematic diagram of the linearizer. The input to the linearizer is divided into two equal quadrature components in a 90° hybrid power splitter. Each quadrature component is applied to a dual-gate FET which is biased for nonlinear operation. The outputs of each dual-gate FET are then combined in an in-phase power combiner and amplified in a power linear amplifier to compensate for the loss encountered in the linearization process.

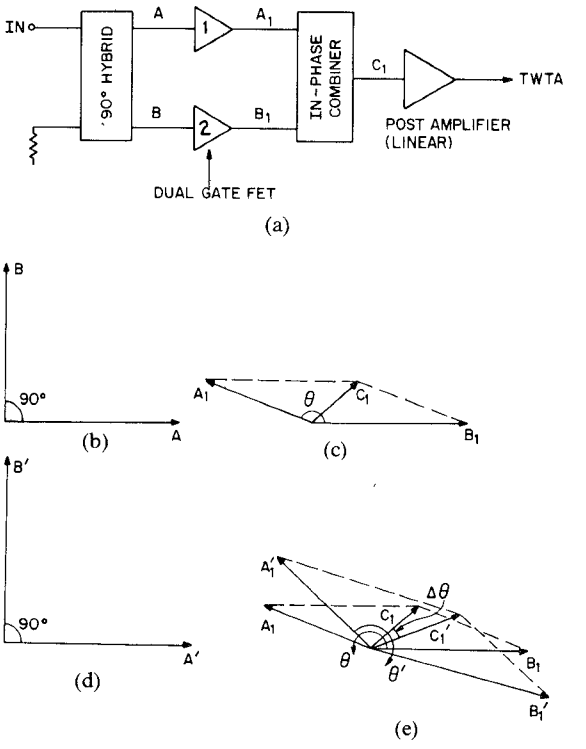

Fig. 2. (a) Schematic diagram of the dual-gate FET linearizer. (b)–(e) Linearizer vector diagrams.

The amplitude and phase of the nonlinearity introduced by the two dual-gate FET's can be controlled by adjusting the dc bias on the second gates. Bias points are chosen to provide simultaneously, a decreasing amplitude attenuation and in increasing phase advance with increasing input power level as monitored at the output of the post-linear amplifier. This is illustrated by the vector diagram representations in Fig. 2(b)–(e) for the circuit shown in Fig. 2(b). Fig. 2(b) shows the two orthogonal vectors $\vec{A}$ and $\vec{B}$ at inputs of the two dual-gate FET's for a particular input power level. The two signals appearing at the output ports of the two dual-gate FET's are A_1 and B_1 as illustrated in Fig. 2(c). The angle between vectors $\vec{A}_1$ and $\vec{B}_1$ is θ, where $\theta > 90°$ ($\theta \sim 160°$). The angle between two vectors increases because of the nonlinearities of the dual-gate FET's. The resultant vector is $\vec{C}_1$ at the output of the in-phase combiner. When the input power increases to a higher level, the input vectors appearing at the inputs of the dual-gate FET's are $\vec{A}'$ and $\vec{B}'$ as shown in Fig. 2(d), where $A' > A$, $B' > B$, and $A'/A = B'/B$. The vectors appearing at the outputs of the dual-gate FET's are $\vec{A}_1'$ and $\vec{B}_1'$ are shown in Fig. 2(e). The angle between vectors $\vec{A}_1'$ and $\vec{B}_1'$ is

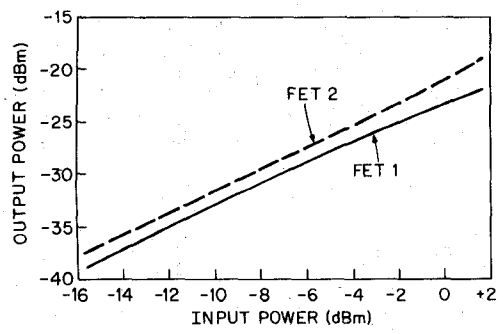

(a)

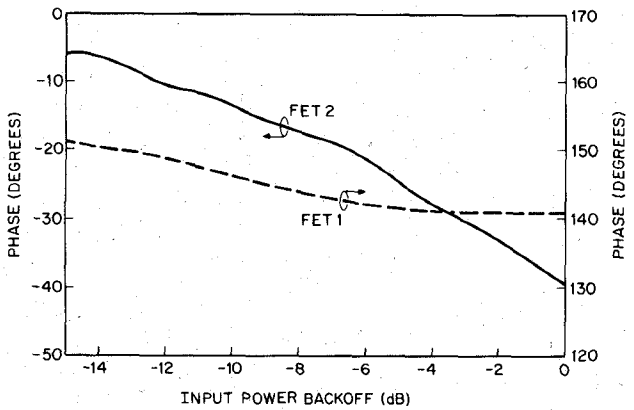

(b)

Fig. 3. (a) Variation of output power of the two dual-gate FET's (Fig. 2(a)) as a function of input power. (b) Variation of output phase of the two dual-gate FET's (Fig. 2(a)) as a function of input power backoff.

θ' and

$$A_1'/A_1 > A'/A \quad B_1'/B_1 > B'/B.$$

The angle between the two vectors $\vec{C}_1'$ and $\vec{C}_1$ is $\Delta\theta$ such that

$$\Delta\theta = \theta' - \theta$$

and

$$C_1'/C_1 > \sqrt{\frac{A'^2 + B'^2}{A^2 + B^2}}.$$

The amplitude transfer characteristics of the two dual-gate FET's are shown in Fig. 3(a). As the input power is increased, there is a gain expansion in both dual-gate FET's. However, FET 1 has more gain expansion than FET 2. The loss in both FET's is about 20 dB. This is because the dual-gate FET's are biased near pinchoff to obtain the nonlinear characteristics. The typical bias voltages on the first gate (RF gate) and second gate (central gates) are -1.5 and -2.5 V, respectively.

The phase relationship between two dual-gate FET's at their outputs (Fig. 2(a)) A_1 and B_1 is shown in Fig. 3(b). The phase difference between these two FET's is about 150° ~ 160°: A 90° phase shift is introduced by the 90° hybrid, and the different nonlinear characteristics of the two dual-gate FET's introduce a phase difference of about 60° ~ 70°. This phase relationship is necessary to obtain proper distortion at the output of the linearizer. This phase relationship introduces additional loss when the two signals are combined in an in-phase combiner. The total loss of the linearizer is about 30–35 dB, which is compensated by the linear amplifier (Fig. 2(a)).

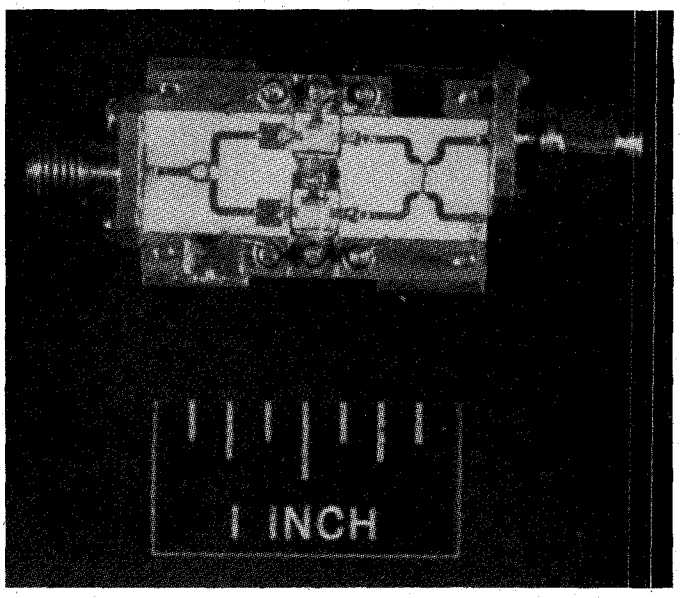

Fig. 4. Photograph of the dual-gate FET linearizer.

Thus, gain expansion and phase advance is obtained as the input power to the linearizer is increased. The amount of phase advance and gain expansion can be adjusted by varying the bias voltages of the two gates of the dual-gate FET's. However, once the bias voltages are adjusted to obtain required improvement in the IMD, they are kept fixed for all power levels. The nonlinearities in amplitude and phase generated by the linearizer are inverse to that generated in the microwave power amplifier.

V. Experimental Results

Two linearizers were designed and fabricated using NEC dual-gate FET's (NE46385) to linearize a *Ku*-band 16-W TWTA and a *C*-band 12-W SSPA. The results of both the TWTA and SSPA with and without linearizers are presented below.

A. TWTA Linearizer

Fig. 4 is a photograph of the dual-gate FET linearizer. Fig. 5 shows the variation of the output power backoff with input power backoff for a single carrier from saturation for a 16-W TWTA with and without linearizer. The curve for the TWTA is plotted at center frequency 11.95 GHz since it does not change with frequency significantly, while curves for the TWTA with linearizer are plotted for different frequencies in the 11.7–12.2-GHz band. The amplitude transfer characteristics of the TWTA with linearizer have better linearity than that of the TWTA alone. The phase transfer characteristics of the TWTA with and without linearizer are presented in Fig. 6. The phase transfer curve for the TWTA is plotted at the center frequency 11.95 GHz. The total phase shift of the TWTA output for a 20-dB dynamic range (0 dB corresponds to saturation) has

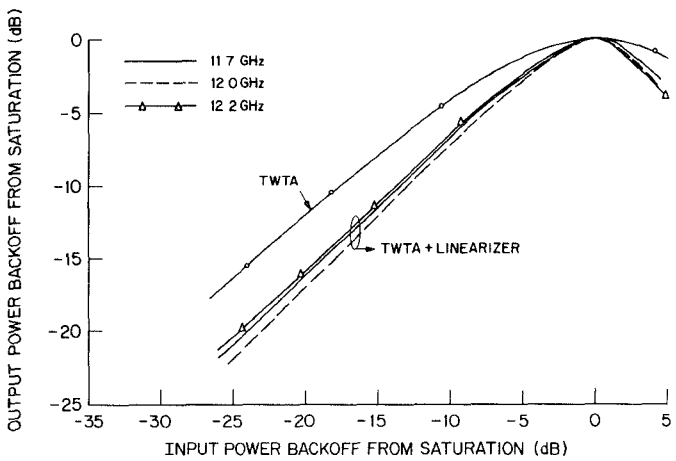

Fig. 5. Output power backoff of the TWTA as a function of input power backoff (0 dB corresponds to saturation).

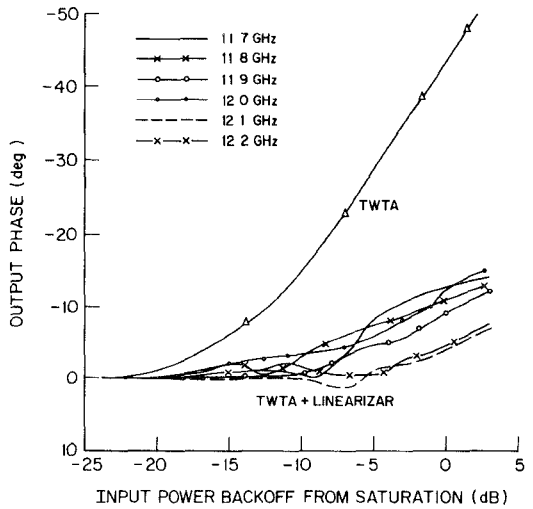

Fig. 6. Output phase of the TWTA as a function of input power backoff from saturation with and without linearizer.

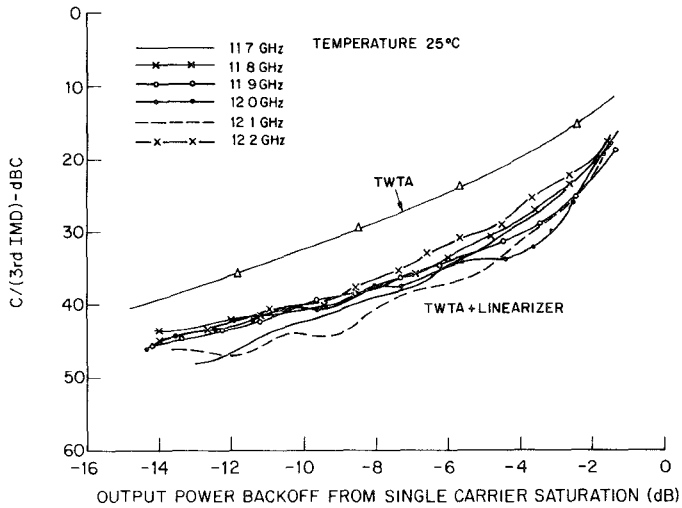

Fig. 7. The C/3rd IMD ratio with and without linearizer as a function of output power backoff at 25°C.

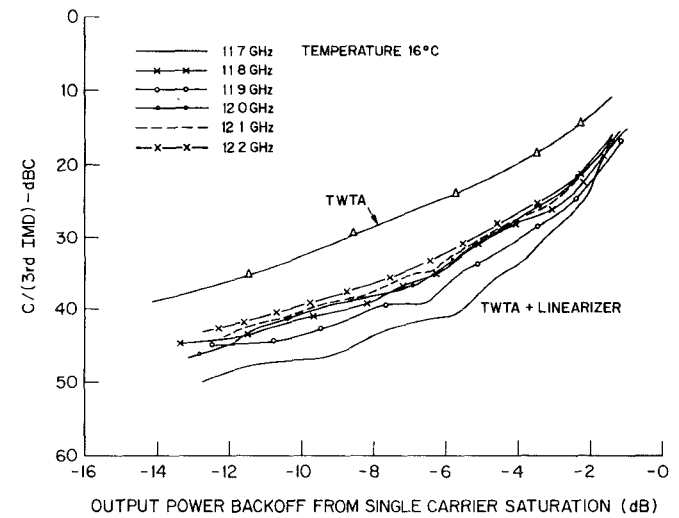

Fig. 8. The C/3rd IMD ratio with and without linearizer as a function of output power backoff at 16°C.

been reduced from 45° to less than 14° over the frequency range of 11.7–12.2 GHz. Thus, there is a considerable improvement in the amplitude linearity (AM-to-AM) and phase linearity (AM-to-PM) of the TWTA by predistorting the input signal to the TWTA.

One measure of improvement in the linearity is the third-order intermodulation distortions generated in the TWTA for a two carrier input signal. Fig. 7 shows the comparison of the performance obtained for a standard TWTA and one that has been linearized using the dual-gate FET predistortion method. In Fig. 7, the C/3rd IMD ratio is plotted as a function of output power backoff from single-carrier saturation for a TWTA at center frequency and for a TWTA with linearizer at frequencies 11.7–12.2 GHz. These results are obtained for two input carriers separated by 5 MHz. Improvements in the C/3rd IMD of 4–5 dB at saturation, 7–12 dB at 4-dB output power backoff have been obtained over 500-MHz band of 11.7–12.2 GHz. An improvement in the C/3rd IMD of more than 7 dB has been obtained over a dynamic range of 10 dB in output power. The linearizer was tested over a temperature range of 15° to 55°.

The results for various temperatures 16°C, 40°C, and 55°C are presented in Figs. 8–10, respectively, for the C/3rd IMD as a function of output power backoff with and without the linearizer. A bandwidth of 400 MHz has been obtained over this temperature range of 15°C to 55°C for very similar improvements in the C/3rd IMD as shown in Fig. 7. The linearizer was tuned at 25°C and 55°C and the bias voltages on the four gates of the two dual-gate FET's are optimized. The bias voltages at 40° are the average of the two sets of bias voltages obtained at 25°C and 55°C. The results indicate that the linearizer can be compensated for temperature variations by using sensistors in the bias circuits.

Figs. 11–14 show the spectrum analyzer display of the output of the TWTA for two input carriers separated by 5 MHz, with and without linearizer, at saturation, 3-dB, 6-dB, and 10-dB output power backoffs from single-carrier saturation. The reduction in the third-order (also fifth and seventh, etc.) intermodulation distortion products is clear from the Figs. 11–14.

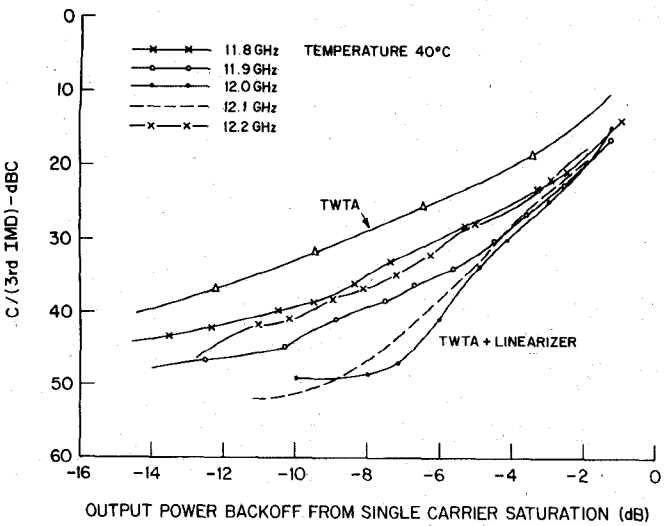

Fig. 9. The C/3rd IMD ratio with and without linearizer as a function of output power backoff at 40°C.

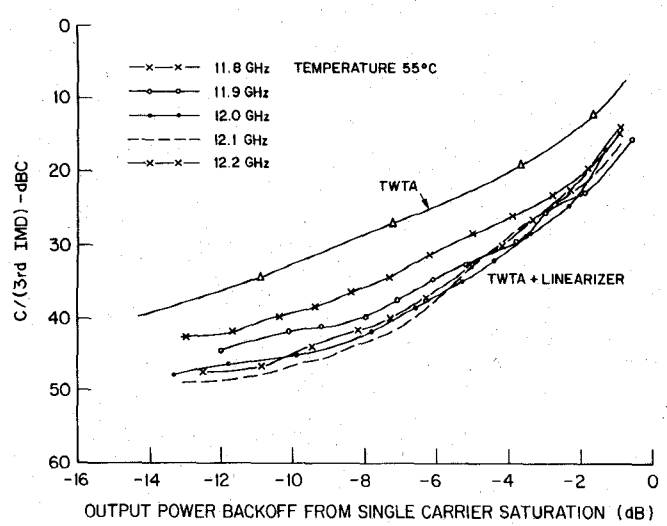

Fig. 10. The C/3rd IMD ratio with and without linearizer as a function of output power backoff at 55°C.

The amplitude transfer characteristics (AM-to-AM) of the linearizer by itself are presented in Fig. 15. The input and output power backoffs are normalized. The linearizer has an insertion loss of about 35 dB over the frequency range 11.7–12.2 GHz. The gain expansion in the linearizer is obvious from Fig. 15. There is a gain expansion of about 1–3 dB over the dynamic range of 20 dB in input power backoffs. The 0-dB input power corresponds to the power required to saturate the TWTA. The phase transfer characteristics (AM-to-PM) of the linearizer by itself are shown in Fig. 16. The input power backoff is normalized, and the 0 dB corresponds to the input power required to saturate the TWTA. The output phase of the linearizer varies about 30° to 50° for an input power range of 20 dB over the 11.7–12.2-GHz range. The phase variation with input power is in opposite directions to that of the TWTA (Fig. 6). Thus, the linearizer produces an inverse phase to that of the TWTA, and the resultant phase variations of the linearized TWTA is reduced as shown in Fig. 6.

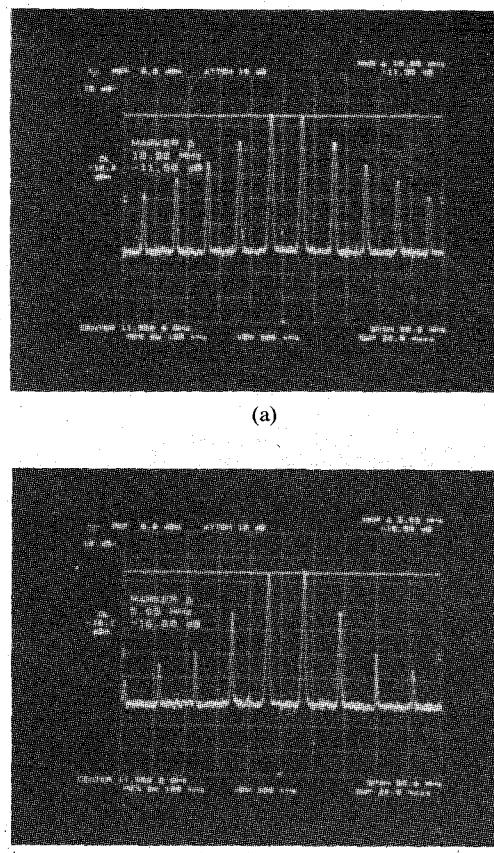

(a) (b)

Fig. 11. Two-tone frequency spectrum of the output of the TWTA at saturation. (a) Without and (b) with linearizer.

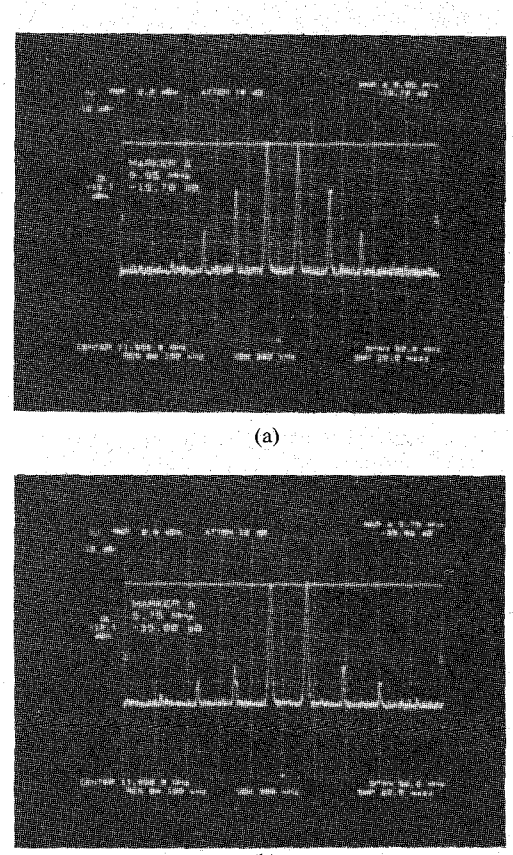

(a) (b)

Fig. 12. Two-tone frequency spectrum of the output of the TWTA at 3-dB output power backoff. (a) Without and (b) with linearizer.

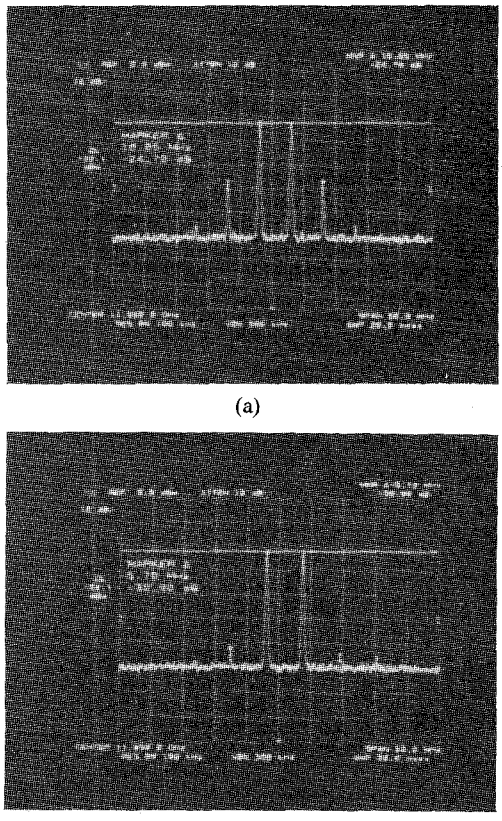

(a) (b)

Fig. 13. Two-tone frequency spectrum of the output of the TWTA at 6-dB output power backoff. (a) Without and (b) with linearizer.

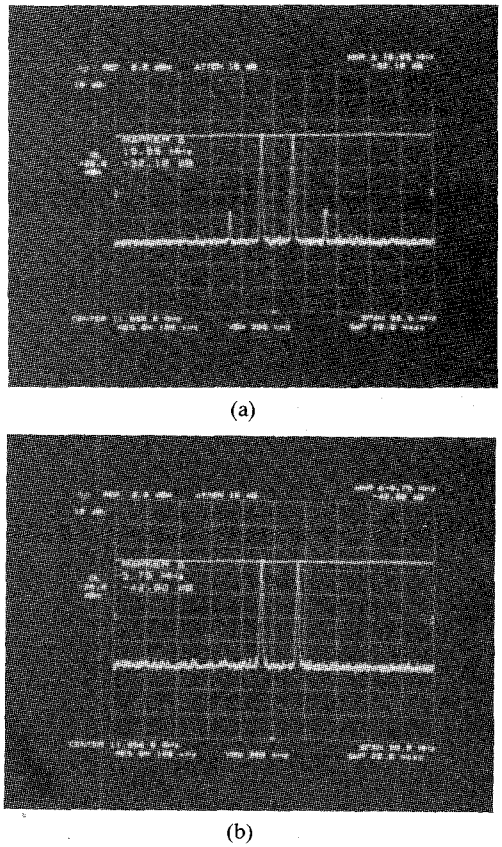

(a) (b)

Fig. 14. Two-tone frequency spectrum of the output of the TWTA at 10 dB output power backoff. (a) Without and (b) with linearizer.

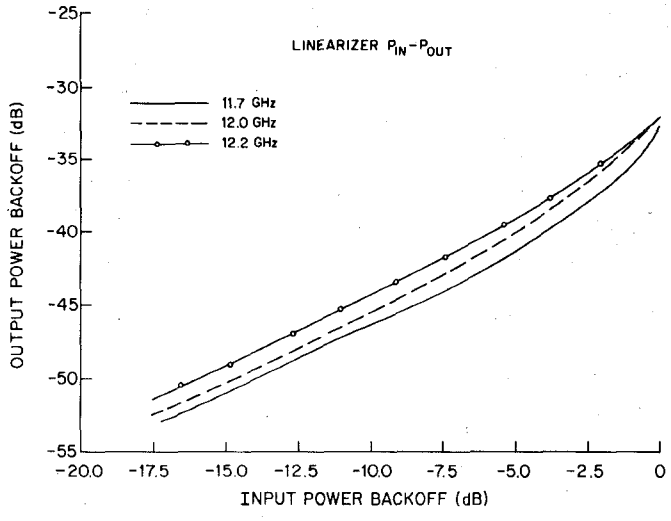

Fig. 15. Normalized output power backoff as a function of input power backoff of linearizer.

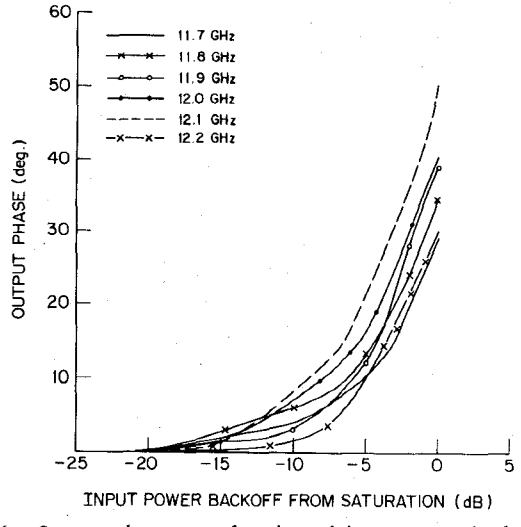

Fig. 16. Output phase as a function of input power backoff of the linearizer.

Video transmission via satellites is being accomplished by using one video signal per channel (transponder). If two video signals are transmitted through one channel (transponder), the undesired chroma crosstalk is high due to the nonlinearities at saturation. To transmit two video signals per channel, one has to use the TWTA's at sufficiently backed-off power levels. Fig. 17 shows the variation of chroma crosstalk as a function of separation of the carrier from the center of the band at saturated output power levels for both with and without the linearizer for a 16-W TWTA at 12 GHz. With the linearizer, the chroma crosstalk has been reduced to less than 1.5 percent, which is within the acceptable limit. Fig. 18 shows the variation of luma crosstalk as a function of input power backoff from saturation with and without linearizer. The separation of the two signals is 12 MHz from the center of the channel, and the IF bandwidth is 24 MHz. IF bandwidth = $2(F + fm)$, where F (8 MHz) is the peak deviation and fm is the upper baseband frequency, (4 MHz for NTSC video). The luma crosstalk is about 4.5 percent at saturation and

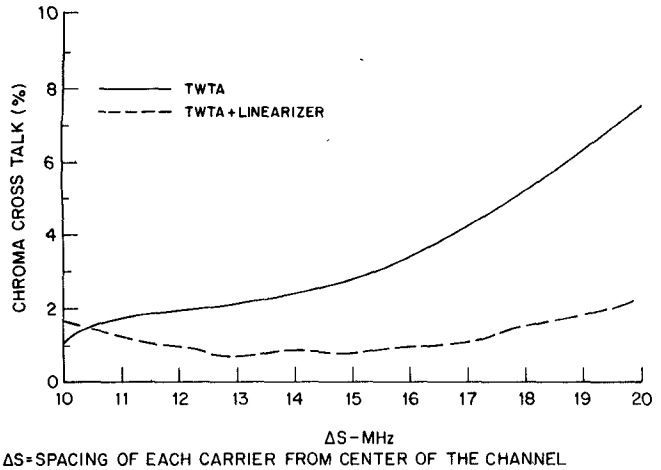

Fig. 17. Chroma crosstalk as a function of spacing of the two carriers from center of the channel.

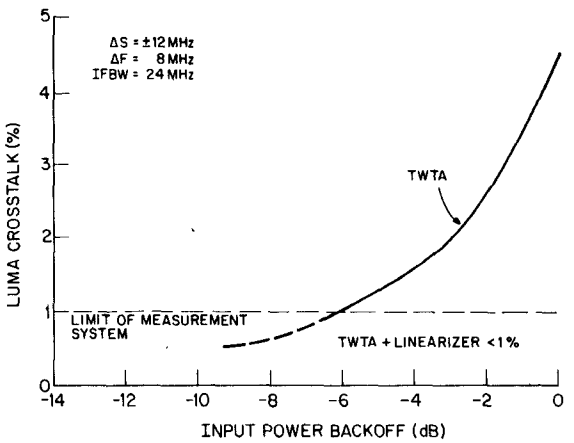

Fig. 18. Luma crosstalk as a function of input power backoff at 12 GHz.

reduces as the input power is reduced. The luma crosstalk has been reduced to less than 1 percent for all power levels including saturated power. One percent is the limit of the measurement system and is an acceptable limit for two carriers to be transmitted in one channel. Thus, by using the linearizer with the TWTA, two video signals can be transmitted through one transponder at saturated power levels. *Thus, performance improvement can virtually double the traffic-handling capability of the satellite.*

B. SSPA Linearizer

A linearizer was also designed and fabricated for linearizing a 12-W solid-state power amplifier operating over 3.7–4.2 GHz. Fig. 19 shows the variation of the output power backoff with input power backoff for a single carrier from saturation (operating point) for a 12-W SSPA. Here, saturation of the SSPA is defined as the operating point where optimum power level and efficiency are obtained. This operating point (saturation) occurs at about 3-dB gain compression point with and without the linearizer over a frequency range of 3.8–4.2 GHz for the SSPA used. The amplitude transfer characteristics (AM-to-AM) of the SSPA with the linearizer have better linearity than that of the

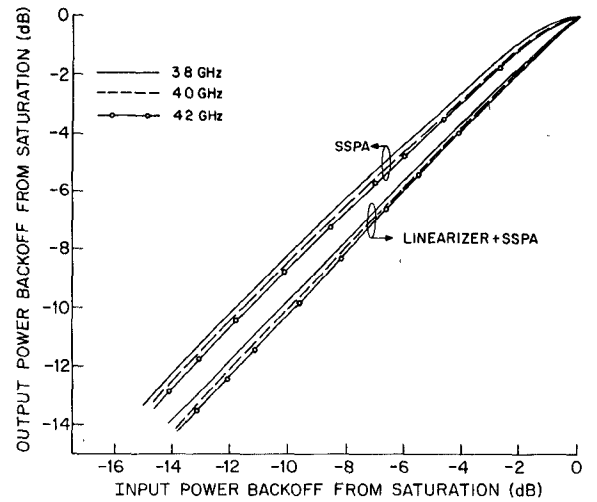

Fig. 19. Output power backoff of the SSPA as a function of input power backoff with and without linearizer (0 dB corresponds to saturation).

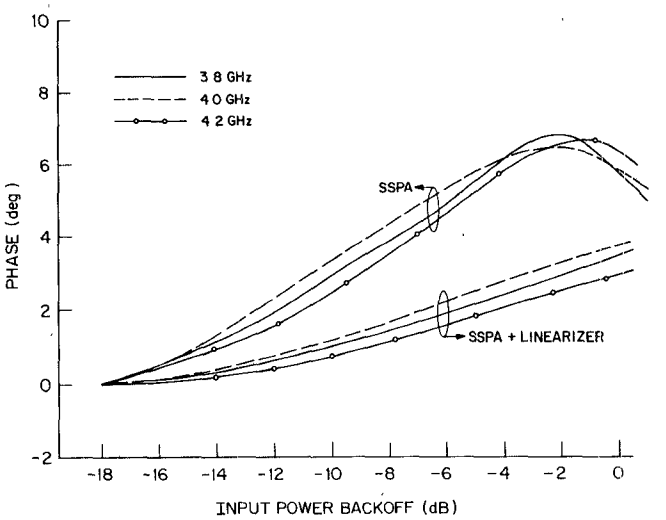

Fig. 20. Output phase of the SSPA as a function of input power backoff from saturation with and without linearizer (0 dB corresponds to saturation).

SSPA alone. The phase transfer characteristics (AM-to-PM) of the SSPA with and without the linearizer are presented in Fig. 20. The total phase shift of the SSPA for a 20-dB dynamic range of input power has been reduced from 8° to 4° over 3.8–4.2 GHz. Thus, there is a considerable improvement in the amplitude linearity (AM-to-AM) and phase linearity (AM-to-PM) of the SSPA by predistorting the input signal to the SSPA.

One measure of improvement in the linearity is the third-order intermodulation distortions generated in the SSPA for a two-carrier input signal. Fig. 21 shows the comparison of the performance obtained for a 12-W SSPA and one that has been linearized using the dual-gate FET predistortion method. In Fig. 21, the C/3rd IMD ratio is plotted as a function of output power backoff from single-carrier saturation for the SSPA with and without the linearizer for the frequency range 3.8–4.2 GHz. These results are obtained for two input carriers separated by 5

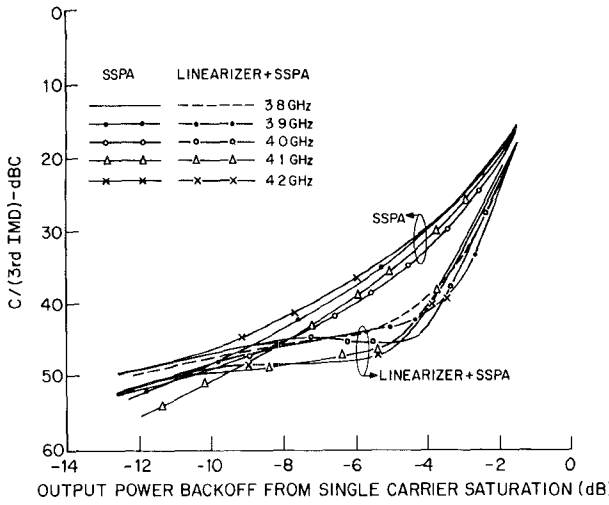

Fig. 21. The C/3rd IMD ratio with and without linearizer as a function of output power backoff.

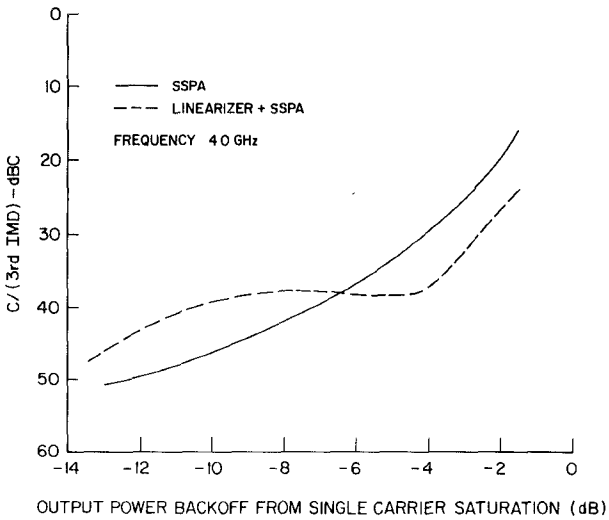

Fig. 22. The C/3rd IMD ratio with and without linearizer as a function of output power backoff.

MHz. Improvements in the C/3rd IMD of 2 dB at saturation, 10 dB at 5-dB output power backoff have been obtained over the 400-MHz band of 3.8–4.2 GHz. Fig. 22 shows the C/3rd IMD ratio as a function of output power backoff from single-carrier saturation for the SSPA with and without the linearizer at 3.95 GHz. In this case, the linearizer was tuned to get the best improvement at saturation. The difference between the results of Figs. 21 and 22 is the different gate bias voltages of the dual-gate FET's. The improvement of about 8 dB is obtained at saturation. Thus, a good improvement in the C/3rd IMD can be obtained either at saturation or over a large dynamic range of output power. Provisions can be made to switch the linearizer for two different types of traffic by a telemetric command to change the bias voltages of dual-gate FET's for optimizing performance.

The amplitude characteristics (AM-to-AM) of the linearizer by itself are presented in Fig. 23. The input and output power backoffs are normalized. The linearizer has an insertion loss of about 35 dB. The gain expansion of the

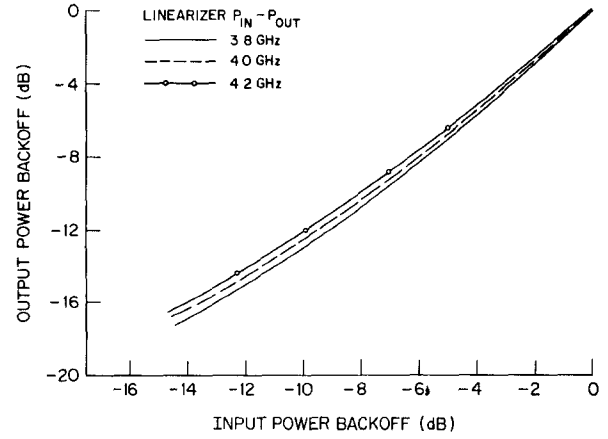

Fig. 23. Normalized output power backoff as a function of input power backoff of the linearizer.

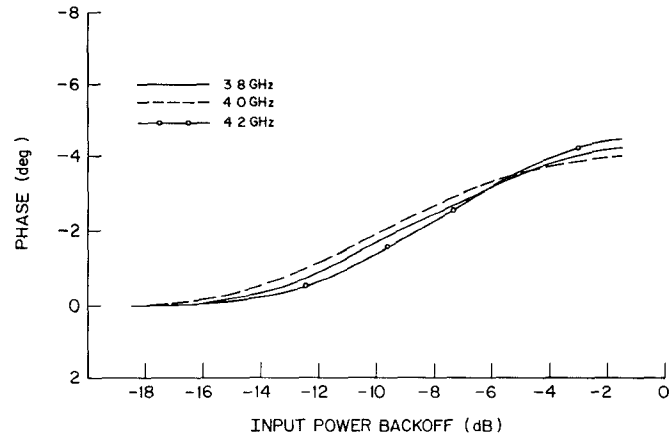

Fig. 24. Output phase as a function of input power backoff of the linearizer.

linearizer is obvious from Fig. 23. There is a gain expansion of about 1 to 2 dB over the dynamic range of 20 dB in input power backoff. The 0-dB input power backoff corresponds to the power required to saturate the SSPA. The phase transfer characteristics (AM-to-PM) of the linearizer by itself are shown in Fig. 24. The output phase of the linearizer varies about 4° for an input power range of 20 dB over 3.8–4.2 GHz. The phase variation with input power is in opposite direction to that of SSPA (Fig. 20). The linearizer produces an inverse phase to that of the SSPA and the resultant phase variation of the linearized SSPA is reduced (as shown in Fig. 20). Figs. 25–28 show the spectrum analyzer display of the output of the SSPA for two input carriers separated by 5 MHz, with and without the linearizer at saturation, with 2-dB, 4-dB, and 6-dB output power backoffs from single-carrier saturation. The reduction in the third (also fifth and seventh, etc.) intermodulation distortion products is clear from Figs. 25–28.

VI. Conclusions

A new predistortion technique is presented for linearizing microwave power amplifiers such as traveling wave tube and solid-state power amplifiers used in satellite transponders and ground stations communication systems.

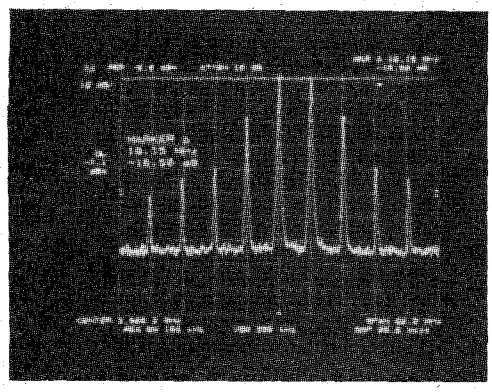

(a)

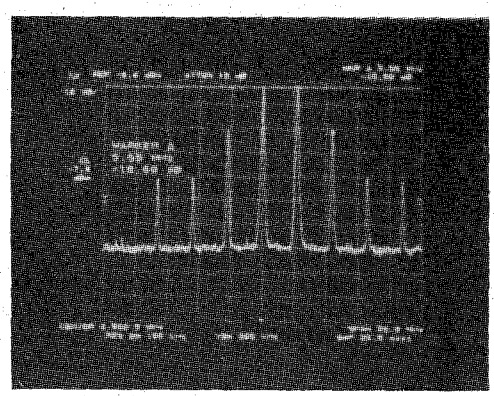

(b)

Fig. 25. Two-tone frequency spectrum of the output of the SSPA at saturation. (a) Without and (b) with linearizer.

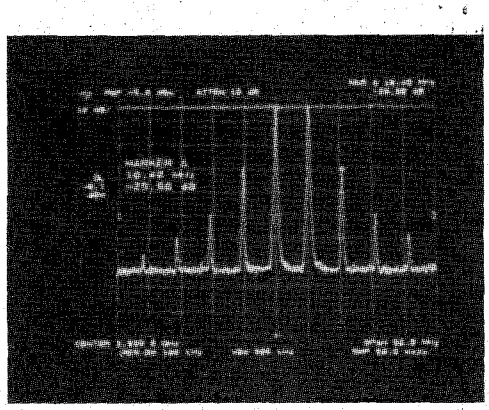

(a)

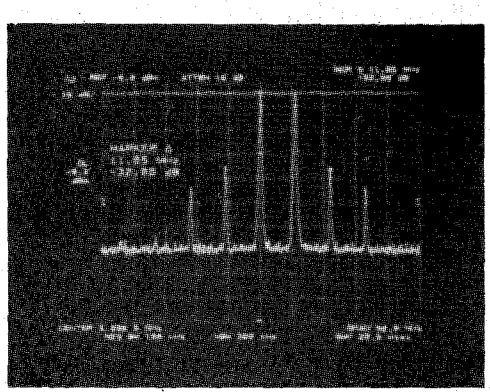

(b)

Fig. 26. Two-tone frequency spectrum of the output of the SSPA at 2-dB output power backoff. (a) Without linearizer and (b) with linearizer.

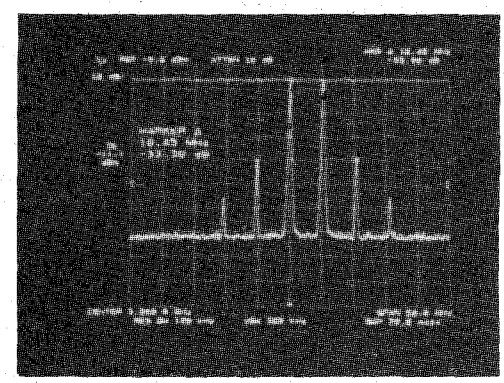

(a)

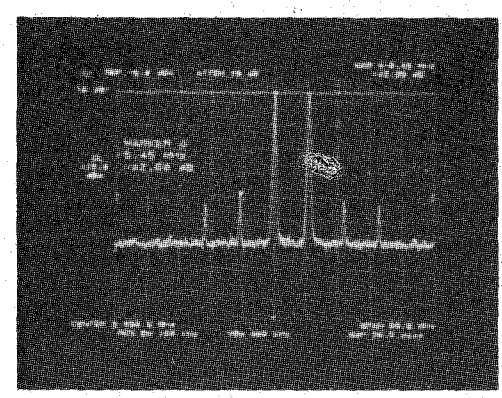

(b)

Fig. 27. Two-tone frequency spectrum of the output of the SSPA at 4-dB output power backoff. (a) Without linearizer and (b) with linearizer.

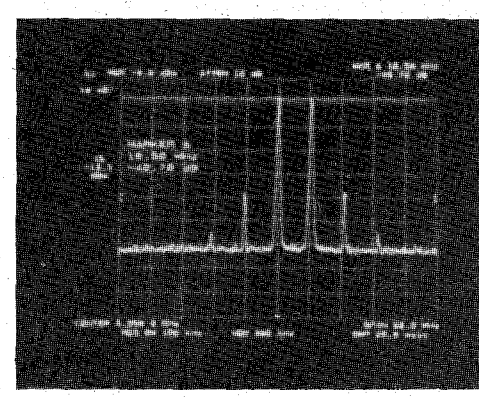

(a)

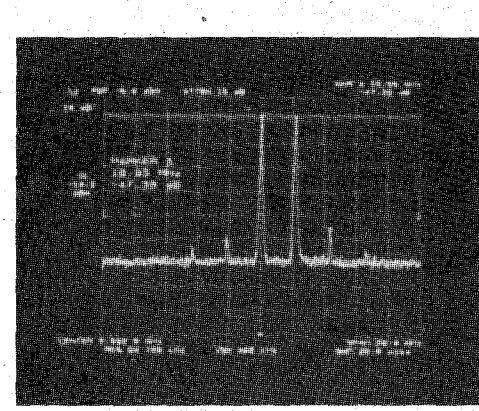

(b)

Fig. 28. Two-tone frequency spectrum of the output of the SSPA at 6-dB output power backoff. (a) Without linearizer and (b) with linearizer.

In this technique, dual-gate FET's are used as nonlinear devices to generate the inverse amplitude and phase nonlinearities to that of the MPA. The results for a linearized 16-W TWTA for 11.7–12.2 GHz, and a linearized 12-W SSPA for 3.8–4.2 GHz are presented. In both cases, very good improvements have been obtained in the C/3rd IMD ratios, and the AM-to-AM and AM-to-PM distortions are reduced. The improvements obtained in the chroma and luma crosstalks obtained with the linearized TWTA at 12 GHz allows the TWTA to be operated at saturation and to double the traffic-handling capacity of the satellite. The circuit for the linearizer is quite simple and is adoptable to different types of TWTA's or SSPA's by changing of the bias voltages of the dual-gate FET's.

Acknowledgment

The authors wish to thank Drs. S. Y. Narayan and Fred Sterzer for motivating technical discussions, support, and encouragement. Thanks are also due to Drs. K. Jonnalagadda and A. Guida for the computer simulation study and to R. Klensch and K. Kelly for cross-talk measurements.

References

[1] M. Sidel, "A microwave feed-forward experiment," *Bell Syst. Tech. J.*, vol. 50, pp. 2879–2961, Sept. 1971.
[2] P. Lubell *et al.*, "Linearizing amplifiers for multisignal use," *Microwaves*, pp. 46–50, Apr. 1974.
[3] C. C. Hsieh and E. Strid, "A *S*-band high power feedback amplifier," in *1977 IEEE MTT-S Int. Microwave Symp.* (San Diego, CA), June 21–23, 1977, pp. 182–184.
[4] J. Namiki, "An automatically controlled predistorter for multilevel quadrature amplitude modulation," *IEEE Trans. Commun.*, vol. COM-31, pp. 707–712, May 1983.
[5] C. Bremenson *et al.*, "Linearizing TWT amplifiers in satellite transponders system aspects and practical implementation," in *Proc. AIAA 8th Commun. Satellite Syst. Conf.* (Orlando, FL), Apr. 20–24, 1980, pp. 80–89.
[6] G. Satoh and T. Mizuno, "Impact on a new TWTA linearizer upon QPSK/TDMA transmission performance," *IEEE J. Select. Areas Commun.*, vol. SAC-1, Jan. 1983.
[7] S. Lenz, "Design and performance of microwave predistortion networks using MIC-technique," in *13th Eur. Microwave Conf.*, (Nurnberg, W. Germany), Sept. 5–8, 1983, pp. 687–692.
[8] G. Sato *et al.*, "A linearizer for satellite communications," in *Conf. Rec. ICC'80*, pp. 33.3–33.3.5.
[9] J. Czech, "A linearized 4 GHz wideband FET power amplifier for communication satellite," in *AIAA Communication Satellite Conf.* (Orlando, FL), Mar. 19–22, 1984, pp. 511–520.
[10] P. H. Charas and J. D. Rogers, "Improvements in on-board TWTA performance using amplitude and phase predistortion," presented at Int. Conf. on Communication, Systems Technology, Apr. 7–10, 1975, IEE, Savory Place, London.
[11] G. R. Welti *et al.*, "Application of predistortion linearization to satellite transponders," in *Conf. Rec., Int. Conf. on Communications*, June 1980, pp. 33.5.1–33.5.2.
[12] D. Cahana, "Practical aspects of predistortion diode linearizers for satellite transponders," presented at 14th Eur. Microwave Conf., Belgium, Sept. 10–13, 1984, Session A1.

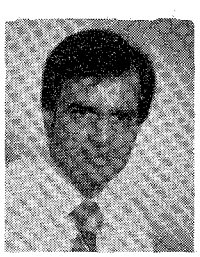

Mahesh Kumar (S'75–M'77–SM'83) received the Ph.D. degree in electrical engineering from the Indian Institute of Technology in 1977.

From 1976 to 1978, he was a Lecturer with the Radar and Communication Center, Indian Institute of Technology. There he engaged in research on the feed for phased-array radar. In 1978, he joined RCA Laboratories, Princeton, NJ, as a Member of the Technical Staff. Since then he has been involved in the research and development of microwave devices, including GaAs FET's, amplifiers, multipliers, linearizers, monolithic dual-gate FET phase shifters, and monolithic switch matrices.

Dr. Kumar has published and presented about 30 papers on, for instance, stripline/microstrip components, FET amplifiers, phase shifters, monolithic microwave integrated circuits, and linearizers. He holds seven patents and six pending.

He is a Past Chairman of the MTT/ED Chapter, PACE, Chairman of the Princeton Section of the IEEE, and currently the Chairman of the Metropolitan Sections Activities Council (METSAC) of the IEEE which coordinates activities of four sections in the New York Metropolitan Area.

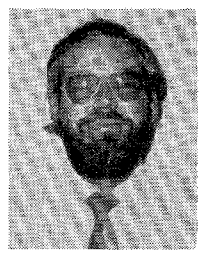

James C. Whartenby (S'79–M'81) received his degree in electronics engineering technology from Trenton State College in 1981.

Upon graduation, he joined the Associate Technical Staff at RCA Laboratories. Mr. Whartenby was involved in the research and development of dual-gate FET amplifiers, monolithic dual-gate FET phase shifters, and microwave power amplifier linearization. In his present position as an Amplifier Production Engineer at Microwave Semiconductor Corporation, he is involved with production support of high-power microwave amplifiers.

Mr. Whartenby has been awarded one patent and has two pending. He has published several papers, one of which was presented at the Sarnoff Symposium of the IEEE Princeton Section. Mr Whartenby is a past PACE Chairman and presently the Membership Development Chairman for the section. He is an adjunct faculty member with the Department of Electronics Engineering Technology at Trenton State College where he regularly teaches courses and laboratories in electronics and RF/Microwave.

Herbert J. Wolkstein (S'49–A'54–M'58–SM'80) joined RCA Microwave Operations in 1955 after seven years as project Engineer in the Research Laboratories of National Union Electric Corporation, where he worked on the design of special-purpose beam-deflection and high-speed computer-switching tubes. In 1958, he became Engineering Leader, and, in 1961, Manager, TWT Design and Development. In 1964, as Manager of Microwave Advanced Product Development, he directed a group in advanced development and applications work on TWTs and solid-state devices. In 1972, he was named Manager of the Advanced Programs and Application Engineering Group. He held that position until 1975; then he became a Member of the Technical Staff of the Microwave Technology Center, RCA Laboratories, Princeton, NJ. In his present position of Manager, Space and Countermeasure Programs, he is engaged in the development and applications of solid-state microwave devices and subsystems.

In 1983, Mr. Wolkstein received a David Sarnoff Award for Outstanding Technical Achievement, RCA's highest honor. He has been awarded 15 patents in microwave TWT and solid-state system designs for presentation at technical conferences and/or publication in technical journals.

Mr. Wolkstein is a member of IEEE's Professional Group on Electron Devices and the Professional Group on Microwave Theory and Techniques.